Quaternary Research 73 (2010) 413–424

Contents lists available at ScienceDirect

Quaternary Research

journal homepage: www.elsevier.com/locate/yqres

Late Quaternary megafloods from Glacial Lake Atna, Southcentral Alaska, U.S.A.

Michael Wiedmer [a,*], David R. Montgomery [b], Alan R. Gillespie [b], Harvey Greenberg [b]

[a] School of Forest Resources, College of the Environment, University of Washington, Box 352100 Seattle, WA 98195, USA
[b] Quaternary Research Center, University of Washington, Seattle, WA 98195, USA

ARTICLE INFO

Article history:
Received 23 July 2009
Available online 31 March 2010

Keywords:
Alaska
Matanuska
Knik
Megaflood
Outburst flood
Lake Atna
Rogen moraines
DeGreer moraines
Pygmy whitefish

ABSTRACT

Geomorphic, stratigraphic, geotechnical, and biogeographic evidence indicate that failure of a Pleistocene ice dam between 15.5 and 26 ka generated a megaflood from Glacial Lake Atna down the Matanuska Valley. While it has long been recognized that Lake Atna occupied ≥9000 km^2 of south-central Alaska's Copper River Basin, little attention has focused on the lake's discharge locations and behaviors. Digital elevation model and geomorphic analyses suggest that progressive lowering of the lake level by decanting over spillways exposed during glacial retreat led to sequential discharges down the Matanuska, Susitna, Tok, and Copper river valleys. Lake Atna's size, ~50 ka duration, and sequential connection to four major drainages likely made it a regionally important late Pleistocene freshwater refugium. We estimate a catastrophic Matanuska megaflood would have released 500–1400 km^3 at a maximum rate of $\geq 3\times10^6$ m^3 s^{-1}. Volumes for the other outlets ranged from 200 to 2600 km^3 and estimated maximum discharges ranged from 0.8 to 11.3×10^6 m^3 s^{-1}, making Lake Atna a serial generator of some of the largest known freshwater megafloods.

Introduction

Catastrophic outbursts from large paleolakes impounded by Quaternary glacial dams are Earth's largest recorded freshwater floods. These megafloods, some only recently recognized (Montgomery et al., 2004; Komatsu et al., 2009), carved and built regional landscapes (Bretz, 1923) and possibly influenced climate change (Teller et al., 2002). Described Alaskan glacial paleolake outburst routes include the Kenai River, inferred from large dunes by Reger et al. (2008); the Tok River (Fig. 1), inferred from depositional evidence by Reger and Hubbard (2009); and the Porcupine River, inferred from erosional and depositional evidence by Thorson (1989). Glaciolacustrine sediments from south-central Alaska's Wisconsin-age (marine oxygen isotope stage [MIS] 2) Glacial Lake Atna (Nichols, 1965) were first reported by Schrader (1900), and subsequent mapping (Nichols and Yehle, 1969; Williams and Galloway, 1986) has revealed a paleolake covering ≥9000 km^2 in what is now the intermontane Copper River Basin (CRB, Fig. 1). Previous attention has focused on Lake Atna's morphology and chronology; the lake's drainage routes and discharge behaviors have received scant scrutiny. Here we report geomorphic, stratigraphic, geotechnical, and biogeographic evidence for a late glacial Lake Atna-sourced megaflood down the Matanuska Valley, a previously unrecognized drainage route, and provide the first estimates for flood volumes and peak discharges through other previously recognized outlets.

The eastern Alaska Range and the Wrangell, Chugach, and Talkeetna mountains encircle the CRB. Throughout the Pleistocene, glaciers from these mountains repeatedly spilled into the basin (Nichols, 1965), blocking drainages, principally the ancestral Susitna and Copper rivers, and impounding large lakes. Latest Lake Atna formed >58,600 ± 1100 ^{14}C yr BP (Ferrians, 1984) and fluctuated in extent before ultimately draining via the Copper River prior to 10,270–11,090 cal yr BP[1] (Rubin and Alexander, 1960). During these glaciations, the Matanuska, Powell, and Nelchina glaciers flowed north from the Chugach Mountain crest to block the entrance and upper reaches of the Matanuska Valley (Fig. 1). Tahneta Pass forms the modern drainage divide between the Copper River to the east and the Matanuska River to the west. Matanuska Valley, a structural trough underlain predominantly by sedimentary, metasedimentary, and plutonic rocks (Winkler, 1992), extends westward from Tahneta Pass to intersect the south-trending Susitna Valley.

Beginning in the late Neogene, multiple glacial advances down the Matanuska Valley merged with Alaska Range glaciers flowing south down the Susitna Valley and descended ancestral Cook Inlet (Manley et al., 2002). During the last major MIS 2 advance, ice from the Matanuska and Knik valleys (Fig. 1) did not merge with the Susitna Valley trunk glacier but terminated at the eastern edge of the Susitna Valley, where it left the prominent Elmendorf Moraine (Fig. 2A). Formation by the Knik Glacier (Fig. 2A) of the southern Elmendorf

* Corresponding author. Current address: U.S. Geological Survey, Forest and Rangeland Ecosystem Science Center, Cascadia Field Station, University of Washington, Seattle, WA 98195, USA.
E-mail address: mwiedmer@u.washington.edu (M. Wiedmer).

[1] All radiocarbon dates ≤21 ^{14}C ka BP have been calibrated with CALIB Rev. 5.0.2, IntCal04 dataset (Reimer et al., 2004) using 1σ values and reported here in calibrated "calendar" years.

0033-5894/$ – see front matter
doi:10.1016/j.yqres.2010.02.005

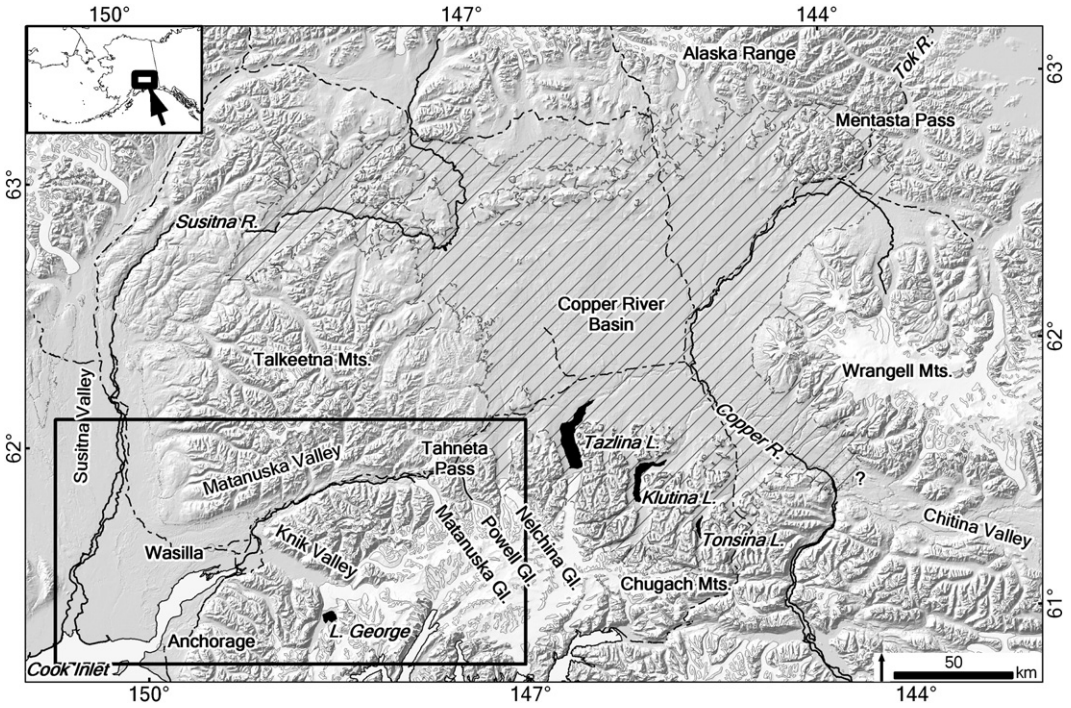

Figure 1. Copper River Basin and Matanuska Valley area, south-central Alaska. Solid rectangle outlines Figure 2A; hatchures indicate the maximum possible extent of Lake Atna's 975-m lake level (see Fig. 4 for further explanation); white shading represents modern glaciers; and dash-dot lines represent the highway system. Query indicates uncertainty regarding the extent of Lake Atna into the Chitina River valley.

Moraine lobe dates to 13,000–17,200 cal yr BP (Reger et al., 1995), whereas formation of the northern lobe by the Matanuska Glacier dates to >14,252 ± 123 cal yr BP (Kopczynski, 2008).

The highest reported Lake Atna sediments are at ~975 m amsl in the northwestern portion of the basin (R & M Consultants, 1981; Williams and Galloway, 1986). Shorelines and deltas in the northwestern and lacustrine-modified terrain in the northeastern CRB indicate the highest prolonged lake elevation is at ~914 m amsl (R & M Consultants, 1981; Schmoll, 1984; Williams and Galloway, 1986). Williams and Galloway (1986) identified an 8-km-wide flow path at ≤975 m amsl from the CRB through Tahneta Pass (907 m amsl) and adjacent Squaw Creek to the Matanuska Valley, and within this broad path they mapped shorelines of a distinct spillway at ~914 m amsl (Fig. 2B). Williams and Galloway (1986) identified neither source nor sink for these drainage patterns; we suspect they resulted from the decanting of the uppermost ~60 m of Lake Atna down the Matanuska Valley by drawing down the 975-m amsl lake surface elevation to 914 m amsl.

In 2008 and 2009, we investigated field evidence for cataclysmic flooding from Lake Atna down the Matanuska Valley. Site elevations were measured with a hand-held GPS (global positioning system) receiver, or surveyed with laser range finders from GPS reading locations. Terrain was modeled from the National Elevation Dataset's 2-arc-second DEM (Digital Elevation Model) for Alaska.

Geomorphic and stratigraphic evidence

Several features along the Matanuska Valley indicate megaflood passage. In unconsolidated CRB deposits immediately east of Tahneta Pass, a series of subparallel curvilinear longitudinal grooves ≤12 km long, ≤700 m wide, and ≤10 m deep converge toward the upper Matanuska Valley (Fig. 2B). These grooves are morphologically similar to those reported for other megaflood routes (Baker, 1978; Gupta et al., 2007) and appear to be confined to elevations below 975 m amsl. If produced by glacial ice, we would expect grooves higher up the valley slopes, not just below maximum lake level.

An isolated streamlined bedrock-cored hill cresting at ~1051 m amsl rises above the Tahneta Pass floor immediately west of the grooved terrain (Tahneta Hill, Fig. 2C). The base elevation of the hill prow is ~914 m amsl, the length:width ratio is 3.2, and scour is apparent on each side of the hill. The elevation of the inflection between the gradually sloping, sediment-draped lower slopes and the steeper, barren bedrock is ~975 m amsl, the maximum reported lake level. Another airfoil-shaped hill stands midway down the valley, with the bedrock stoss (up-valley) side nearly vertical and till-mantled lee side gradually sloped (Fig. 2D). The length:width ratio of 3.2 and position of greatest width 2/3 the distance between the lee and stoss ends of this hill correspond to flood-formed islands (Komar, 1983; Gupta et al., 2007). Crescentic scour on the upstream side, an oblique channel crossing the longitudinal crest, and downstream tapering streamlines on the adjacent channel floor are features typical of similar "islands" in Washington State's Channeled Scablands (Baker, 1978). Both Matanuska Valley streamlined hills are on local topographic highs, have no sediment on their upper surfaces, and are in confined valleys where glacial flow would be rapid. If these hills were glacially formed crag-and-tail drumlins, we would expect length:width ratios of ~10+ (Briner, 2005; Kerr and Eyles, 2007). Although absence of both till and recessional moraines through the middle reaches of the Matanuska Valley (Williams, 1986) is consistent with flood scour (Fig. 2A), it is also consistent with catastrophic disruption prior to significant glacial recession.

A prominent sequence of approximately 25 large flow-transverse ridges (Fig. 2E) lies west of the city of Wasilla within a >100 km^2 area of deep (>100 m; Reger and Updike, 1983) unconsolidated deposits at

Figure 2. A: Matanuska Valley flood route. B: Tahneta Pass area: arrows and dashed lines show previously mapped (Williams and Galloway, 1986) broad flow path and discrete spillway with no reported source or sink. C: Tahneta Hill. D: streamlined hill (QuickBird images ©Digital Globe, 2005). E: 2-D symmetric very large subaqueous dunes (VLD); Q_A = Quaternary alluvium, Q_D = Quaternary Matanuska megaflood VLD train, Q_K = Quaternary Knik Glacier post-flood advance, Q_O = post-flood trough-filling Knik Glacier outwash, F represents location of exposure. F: VLD exposure with foreset beds dipping 18–25° to the right. Large arrows in C–F show direction of flow during the flood.

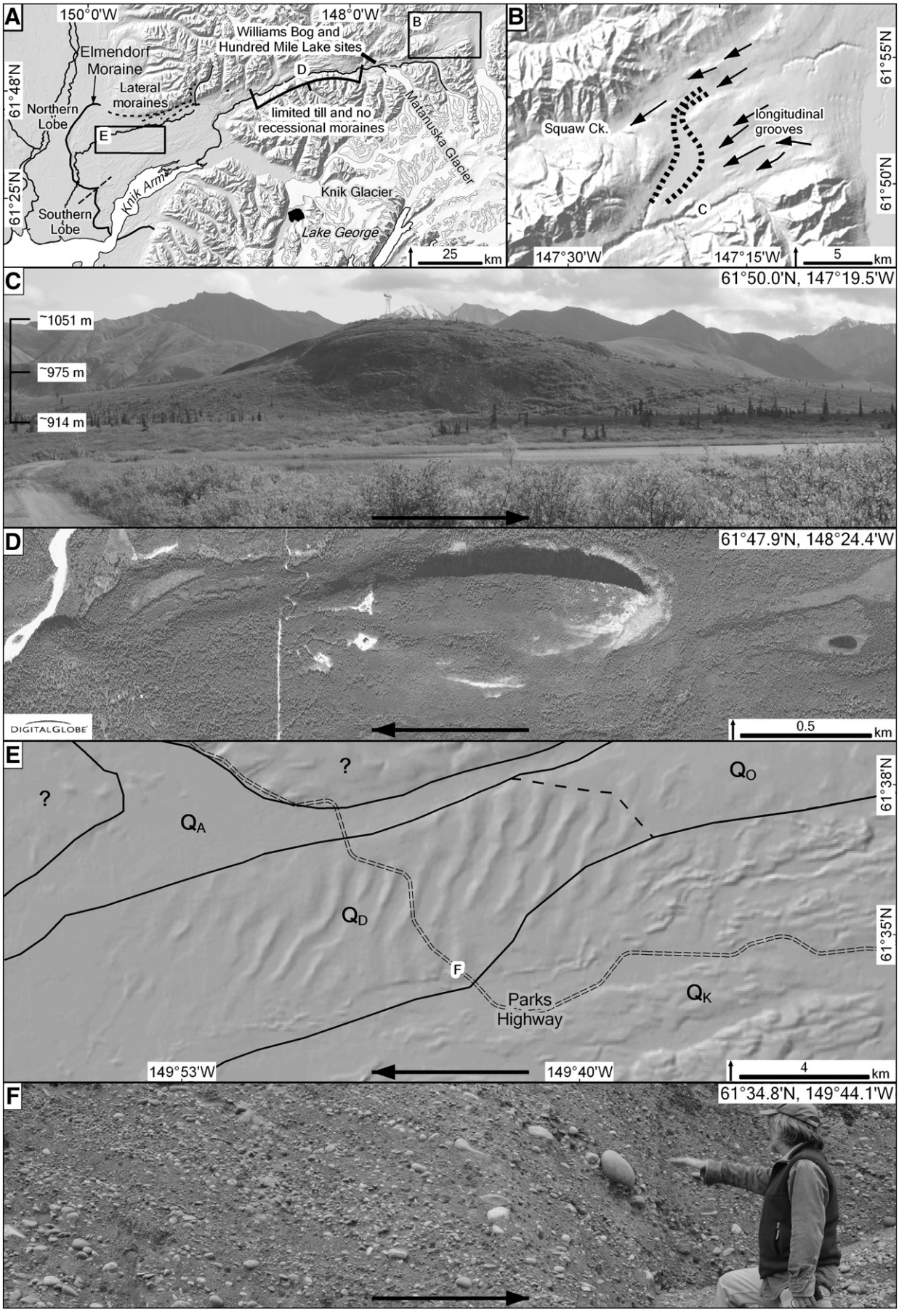
A
150°0'W
148°0'W
61°48'N
61°25'N
Elmendorf Moraine
Lateral moraines
Northern Lobe
Southern Lobe
Knik Arm
Williams Bog and Hundred Mile Lake sites
B
D
E
limited till and no recessional moraines
Matanuska Glacier
Knik Glacier
Lake George
25 km
B
61°55'N
61°50'N
Squaw Ck.
longitudinal grooves
C
147°30'W
147°15'W
5 km
C
61°50.0'N, 147°19.5'W
~1051 m
~975 m
~914 m
D
61°47.9'N, 148°24.4'W
DIGITALGLOBE
0.5 km
E
?
?
Q_A
Q_O
Q_D
Q_K
61°38'N
61°35'N
F
Parks Highway
149°53'W
149°40'W
4 km
F
61°34.8'N, 149°44.1'W

the confluence of the Matanuska and Susitna valleys. The best-preserved ridges decrease progressively in height from 34 m (up-valley) to 5 m (down-valley), have crestlines running ≤7 km, with occasional Y-junctions, and mean crest-to-crest distances of 0.89 ± 0.15 km (Fig. 3). They are relatively symmetric in cross section (mean stoss and lee angles of 2.1 ± 0.8° and 2.3 ± 0.8°), and have smoothed and rounded crests, and cross sections appear similar along individual crestlines. One (Fig. 2F) of the several borrow pits recently developed in the area exposes the internal stratification of one ridge, revealing ~2 m of surficial subhorizontal fluvial sand to cobble beds nonconformable with the ridge surface. These subhorizontal beds unconformably overlie a >5 m packet of clast-supported clean sand to cobbles including foreset beds dipping 18–25° down-valley (west). These foresets include occasional subangular boulders >1 m in diameter. Some layers are washed, with open architecture infiltrated with silt, and the bedform surfaces are not armored with large clasts. Fluvial sediments are exposed throughout the pit: ≤10 m below the surrounding ground surface, >200 m normal to, and >130 m parallel to the ridge crestline.

Superposed on the large ridges are hundreds of smaller (≤3 m high) subparallel ridges, symmetrical in cross section and uniform in intra- and inter-ridge morphology. These smaller ridges are spaced ≤100 m apart, are constructed of well-washed poorly bedded gravelly alluvium (Reger and Updike, 1983), and are on both the stoss and lee slopes of the larger subjacent ridges. Their crestlines occasionally merge and intersect. The sorting and clast support of the sediments indicate a fluvial rather than glacial origin. Nevertheless, these superposed ridges have been interpreted as crevasse-fills (Trainer, 1953) or annual recessional (DeGreer) moraines (Reger and Updike, 1983). Analysis of QuickBird satellite images, however, reveals that the general distribution and individual orientation of these smaller ridges coincide with the large subjacent ridges (Fig. 4), implying a common genesis.

In light of the overall morphology, internal structure, and spatial congruence, we interpret the set of smaller and larger ridges as large subaqueous dunes superposed on very large subaqueous dunes (VLDs), collectively, 2-D symmetric very large compound subaqueous dunes (Ashley, 1990). The central well-preserved VLD morphology follows Allen's (1963) empirical height:slope (his Fig. 4) and mean dune height vs. mean dune-chord relationships (Allen, 1968). Foreset dip angles match those described for other megaflood dunes (Baker, 1978; Rudoy and Baker, 1993) and dune-crest rounding and symmetry have been related to high near-bed flow velocity and high sediment transport rates (Kostaschuk and Villard, 1996). VLD trains are characteristic of glacial lake outburst-flood routes (Baker, 1978).

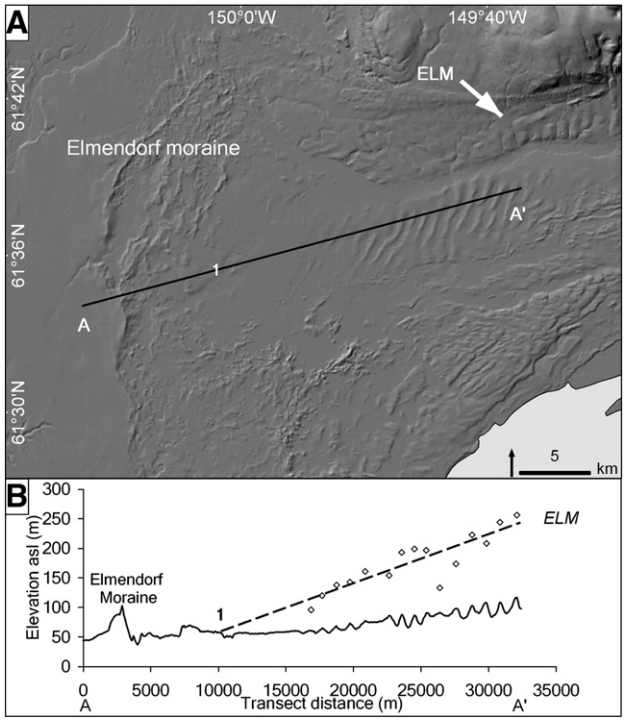

Figure 3. Wasilla-area very large dune (VLD) train and maximum estimated flood water surface elevation, based on Allen's (1968) empirically derived equation relating dune height H and water depth D: $H = 0.086D^{1.19}$ (units in feet). Note that Allen's regression is calculated from dune heights of 0.07 to 8 m, whereas we apply the regression to dune heights of 5 to 27 m. A: Transect A–A' was selected to optimize characterization of the full VLD train and does not represent the flow path. (1) Location on the transect of the intersection of the estimated flood surface level and the modern ground surface (Fig. 3B). ELM = elevation of transition along the truncated right-lateral recessional moraine from a sharp crested form (above) to a smooth, apparently eroded form. B: The solid trace is the topographic contour of transect A–A' (note 1:45 vertical exaggeration); points are calculated flood heights based on individual trough–crest elevation differences using equation above; dashed line is the linear regression through the calculated points ($r^2 = 0.77$, $p < 0.0001$). Water-surface elevation calculated as flood depth above local mean ground surface elevation.

Discussion

Trainer (1953) noted bedded gravels mantling the VLDs west of Wasilla, but he attributed these landforms to alternating zones of debris-laden and clean ice in the ancestral Matanuska Glacier. The extensive exposed fluvial sediments and the linear trend in decreasing ridge height, however, are not consistent with deposition of glacier-borne debris. The VLDs have also been mapped as Rogen moraines (Reger and Updike, 1983), subglacially formed ridges arrayed orthogonally to ice movement. However, Rogen moraines are characterized by gradual transitions between ridges and drumlins; typically have distal crescent-shaped margins, terminal ridge horns pointing down-valley, and fluted and/or hummocky surfaces; and usually occur in areas with near-surface bedrock (Lundqvist, 1989). Unlike the VLDs near Wasilla, Rogen moraines are composed of diamicton, including coarsely bedded debris-flow sediments (Lundqvist, 1989; Fisher and Shaw, 1992); where crude bedding from inferred subglacial flow occurs, it conforms to moraine slopes (Fisher and Shaw, 1992).

Exposed VLD alluvium contains coal and frequent granitic clasts, indicating a Matanuska Valley origin (Winkler, 1992). However, the occasional embedded large angular boulders, the abundance of which appears to decrease northward, are flyschoid metasedimentary clasts of Knik Valley origin (Winkler, 1992; C. Hults, USGS, Anchorage, AK, personal communication, 2009). The angularity of these clasts indicate short transport distances; we speculate that they were stripped from what was then the nearby Knik Glacier lateral moraine by the floodwaters.

Superposed dunes are also apparent on East Wenatchee's Pangborn Bar along the Glacial Lake Missoula flood route (R. B. Waitt, USGS, Vancouver, WA, personal communication, 2009). Analyses of modern river bedforms suggest superposed dune morphology is generated during rapidly decreasing discharges where the formation of small dunes on the previously smooth backs of larger ones would be consistent with transitions in flow regimes. During these transitions, the heights of large depositional dunes are reduced and their crest rounded (Allen and Collinson, 1974). We speculate that the observed upward transition from steeply dipping foresets to subhorizontal beds in the VLDs reflects a flow-regime transition during the waning stages of the flood. In large modern rivers, where two transverse bedform orders are preserved, they differ in scale by approximately one order of magnitude (Allen and Collinson, 1974). In height and chord length, the two orders of dunes near Wasilla also differ by one order of magnitude. As with the Missoula dunes (Baker, 1978), the chord length for the Wasilla-area VLD train increases southward toward the deepest (highest velocity) portion of the flood path (Fig. 5).

In response to isostatic depression of the Cook Inlet–Susitna Lowlands, marine and estuarine waters transgressed into the Anchorage

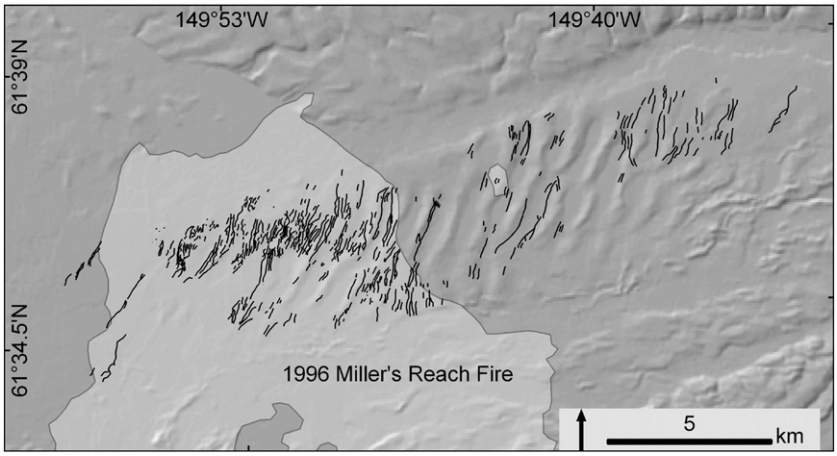

Figure 4. Wasilla-area very large dune (VLD) train and superposed smaller ridges (arcs). We mapped superposed smaller ridges visible in QuickBird (©Digital Globe, 2004) satellite images, selecting ~10-m-wide ridges subtransverse to the Matanuska Valley orientation. The massive 1996 Miller's Reach fire (pale shaded area; AFS, 1999) removed much of the closed mixed forest canopy from the distal end of the VLD train, allowing better visibility of the superposed ridges.

area as glaciers receded, depositing ≥60 m of unconsolidated clays, silts, and sands comprising the Bootlegger Cove Formation (BCF; Updike and Carpenter, 1986). Anchorage lies on the south shore of Knik Arm (Fig. 5), opposite the mouth of the flood path. Seven recognized BCF facies developed in response to energetic fluctuations of the depositional environment. Six of these facies are widely distributed across the Anchorage peninsula, and one, sensitive cohesive silty clay Facies III (>14 ka; Updike et al., 1988), has distinctive geotechnical and geologic characteristics and appears restricted to a laterally continuous ≥7 km by ≥1 km band along Knik Arm (Updike and Carpenter, 1986; Updike and Ulery, 1986; Fig. 5).

Unlike the other facies, mapped Facies III forms a nearly horizontal, thin (<10 m), continuous stratum (Updike and Ulery, 1986). Within Facies III is an open-flocculated "card-house" zone of clay particles with randomly dispersed silt grains (Updike et al., 1988). Widespread collapse of this card-house microfabric during the magnitude 9.2 1964 Alaskan earthquake caused catastrophic Anchorage landslides. Borehole tests demonstrate that pore-fluid composition (mean organic carbon concentration 65 ± 37 ppm, mean chloride concentration 28 ± 26 ppm) within the remainder of the BCF strata (measurements over ~20 m) indicates marine or estuarine deposition, but pore-fluid composition (organic carbon concentration low of 0 ppm, chloride concentration low

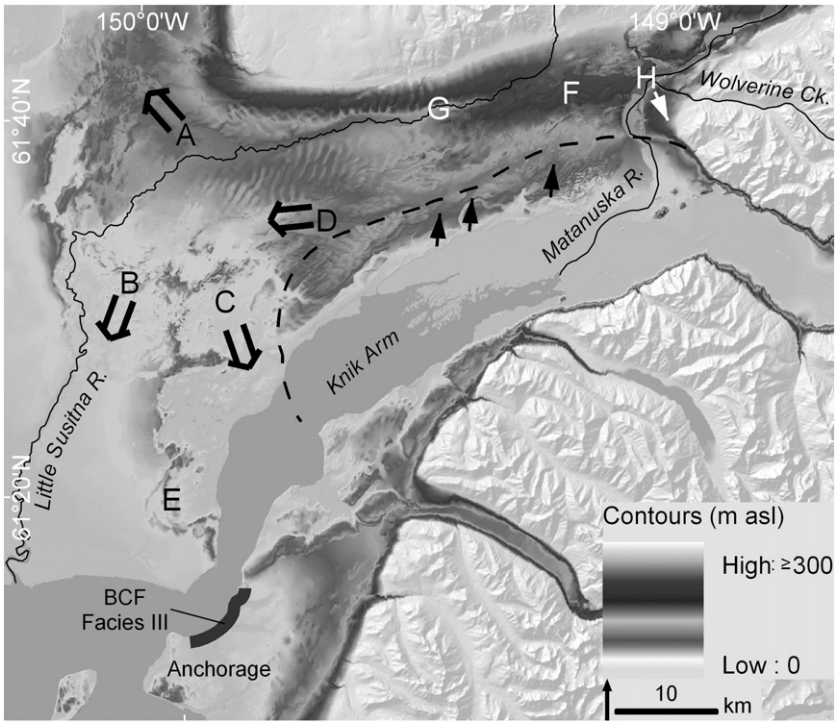

Figure 5. Contour map of lower Matanuska Valley. A–C: flood paths through the Elmendorf Moraine, inferred from stratigraphic (Fig. 8) and topographic evidence and calculated maximum flood surface elevations (Fig. 3). D: post-flood paleochannel along the northern paleo-Knik Glacier margin (approximated by dashed line). E: Knik Glacier readvance terminal moraine, inferred from stratigraphic (Fig. 8) and topographic evidence. F: inferred river mouth bar, with fosse (G) now occupied by the Little Susitna River, the course of which deviates around the bar and VLD train. Fossae are common features of megabars within Washington State's Channeled Scablands (Bretz et al., 1956; Waitt et al., 2009). H: location of foresets (15–20° dip; direction ~160° (white solid arrow)) along the southern wall of Wolverine Creek canyon, which we infer as an outburst flood bar contiguous with the bar at F and later incised by the Matanuska River. Black solid arrows point to locations where the paleochannel is perched above slopes descending to the south, suggesting the Knik Glacier had advanced into Knik Arm, where it formed the southern bank of the active paleochannel. The broad arc in the lower left indicates the general mapped distribution of BCF Facies III.

of 6 ppm) within a specific zone (≤2 m thick) of Facies III suggests a freshwater origin (Updike et al., 1988). In contrast to frequent observations that low-salinity zones in marine clays result from post-depositional leaching (Bjerrum, 1954; Torrance, 1979; Carson, 1981; Woodley, 1996), Updike et al. (1988) noted that the position of the thin BCF low-salinity zone is not stratigraphically consistent with leaching by percolating meteoric water and speculated that an unknown geochemical reaction might be responsible. We likewise speculate that the open-flocculated card-house microfabric associated with nonmarine pore water (non-salt flocculation; *sensu* Lambe, 1958) within BCF Facies III is the fingerprint of turbulent influx of Lake Atna megaflood waters into ancestral Cook Inlet. Paleo-Cook Inlet waters may have been confined by tidewater glaciers descending from multiple directions (Schmoll et al., 1999), thereby limiting downstream sediment distribution. Multiple isolated strata of Facies III are mapped (Updike et al., 1988), possibly reflecting distinct flood events. Better age control of BCF Facies III and Lake Atna floods will help resolve our speculation.

Biogeographic evidence provides additional support for a paleofluvial connection between Lake Atna and Cook Inlet. Pygmy whitefish *Prosopium coulterii* is a nonanadromous species with a strikingly disjunct distribution in north-central and northwestern North America (Fig. 6A; Eigenmann and Eigenmann, 1892; Myers, 1932; Wynne-Edwards, 1947; Eschmeyer and Bailey, 1955; Heard and Hartman, 1966; McCart, 1970; Lindsey and Franzin, 1972; Weisel et al., 1973; Poe et al., 1976; Bird and Roberson, 1979; Russell, 1980; Buell, 1991; Chereshnev and Skopets, 1992; Lonzarich, 1992; Mayhood, 1992; Hallock and Mongillo, 1998; Nelson and Shelast, 1998; Mathisen and Sands, 1999; Mackay, 2000; Rankin, 2004; Plumb, 2006; Zemlak and McPhail, 2006; Froese and Pauly, 2009). Pygmy whitefish typically inhabit cold, deep lakes and glacially fed rivers, most within the footprint of the Laurentide and Cordilleran ice sheets, and morphological variations among populations have been used to infer locations of Pleistocene freshwater refugia (e.g., Lindsey and Franzin, 1972). In Alaska, pygmy whitefish previously were reported only in Copper River and southwestern drainages. Pygmy whitefish are documented, as a result of extensive regional salmon habitat inventories (e.g., Roberson et al., 1978), in three Lake Atna remnants: Tazlina, Klutina, and Tonsina lakes (Fig. 1; Bird and Roberson, 1979). In 2005, MW collected pygmy whitefish in Lake George, a proglacial lake in the Knik Valley which is tributary to the Matanuska Valley. In spite of extensive surveys of likely habitats (e.g., Bill et al., 1972; Barton and Barrett, 1973; ADF&G, 2009a,b), Lake George provides the only known pygmy whitefish habitat in the entire Cook Inlet basin. Considering the topographic barriers between other potential sources (e.g., south-west Alaska), the most likely origin of the Lake George population was Lake Atna via one of the paleolake's western drainages. This interpretation is supported by a multivariate analysis of meristic characters of North American populations, which shows closer phenotypic similarity between the Lake George population and those in CRB lakes than to other Alaskan populations (Figs. 6B, C; Tables 1–3). The observed distribution of pygmy whitefish does not require a paleoflood *per se*, but it does indicate drainage connections between the CRB and the Knik Valley that are no longer extant.

Lake Atna extent estimations

Three Lake Atna outlets (Susitna River, Mentasta Pass/Tok River, and Copper River; Figs. 1, 7) have been previously recognized, based on observed fluvial morphology and prominent shorelines corresponding to pass and spillway elevations (Schmoll, 1984; Williams, 1989), but discharge volumes and fluxes through these outlets have not been estimated. The volume of Lake Atna available to decant down each outlet can be only approximated because of uncertainty of CRB ice-front locations coeval with discrete discharges. For key lake levels reported previously (Ferrians and Schmoll, 1957; Nichols and Yehle, 1969; Williams, 1989), we determined Lake Atna volumes for two bounding conditions: (1) no ice in the CRB except at inferred ice dams (at passes or the limits of recognized glaciolacustrine deposits; Fig. 7A); and (2) with a CRB ice front at the last glacial maximum (LGM; Fig. 7B; Manley et al., 2002). We estimated volumes from the elevation difference between a DEM of the area interior of ice dams and/or the LGM ice front and elevations of the reconstructed lake levels (Table 4). Based on a lake-surface elevation of 975 m amsl, Lake Atna covered 8900–24,000 km^2, was ~60-m deep at Tahneta Pass, and 500–1400 km^3 were available to decant. The volume available to decant down the Susitna Valley was approximately twice as large (1000–2600 km^3), given the greater depth estimated at the dam (Table 4).

We assume that when Lake Atna decanted through the Susitna River outlet (Fig. 7), the northwest basin east to Tyone Spillway drained. The dam height was 346 m [difference between lake surface (914 m amsl) and lowest adjacent mapped lake sediments (~550 m amsl; R & M Consultants, 1981)], the remainder of the basin drained to 777 m amsl (controlled by the Tyone Spillway), and then rapidly lowered to a stable 747 m amsl elevation (Nichols and Yehle, 1969). We assume that Lake Atna drained through Mentasta Pass at an elevation of 701 m amsl and that post-drainage alluvial fan deposition has raised the modern pass elevation to 716 m amsl.

Chronology

The most recent lake levels high enough to decant down the Matanuska and Susitna outlets occurred between 15,170–16,290 (Rubin and Alexander, 1960) and 25,331–26,700 cal yr BP (Thorson et al., 1981; Danzeglocke et al., 2010). The oldest dates for an ice-free upper Matanuska Valley are 15,300–15,640 cal yr BP at Williams Bog (Williams, 1986) and ~15 ka at Hundred Mile Lake (Walker et al., 2005; Fig. 2A). Thus it appears that the flood down the Matanuska Valley occurred between ~15.5 and 26 ka. Lake Atna levels subsequently dropped below the Mentasta Pass elevation prior to ~13,300–13,900 cal yr BP (Ager and Brubaker, 1985).

A large post-flood paleochannel, veneered with till, bounds the southern margin of the Wasilla-area VLDs and is locally perched above Knik Arm to the south (Fig. 5). Outwash deposited by a northward flow partially fills troughs of the easternmost VLDs (Fig. 2E). These features indicate the Knik Glacier remained near its last maximum during the Matanuska flood, likely forming the flood's southern bank. Post-flood, the eroded Knik Glacier spread northward to reoccupy partially the scoured void and westward to the Elmendorf Moraine (Figs. 5, 8). Gravel ridges of fluvial Matanuska gravels, parallel and immediately adjacent to the paleochannel flow and locally capped by Knik till, resemble and have been interpreted as kame–esker complexes (Reger and Updike, 1983). However, they even more closely resemble “boulder berms” (*sensu* Carling, 1989). This latter interpretation is consistent with our flood model, in which they would be deposited after the formation of the VLDs. Other lower Matanuska Valley features attributed (Reger and Updike, 1983) to stagnant ice processes may have resulted from the Knik Glacier readvance or may represent areas where Matanuska Glacier ice survived the flood waters. Reger and Updike (1983) also postulated that the Knik lobe remained active after the Matanuska lobe, but Kopczynski (2008) reached the opposite conclusion. Evidence of disruption of the Matanuska Glacier by floodwaters may help resolve ongoing controversy surrounding its apparently anomalous retreat relative to the adjacent Knik Glacier (Williams, 1986; Reger et al., 1995).

In summary, we suggest this general sequence: 1) both the Matanuska and Knik glaciers began their retreat from the Elmendorf Moraine; 2) a Tahneta Pass ice dam failed 15.5–26 ka, allowing Lake Atna flood waters to descend the Matanuska Valley and disrupt extant glacial ice, while the Knik Glacier remained partially extended into the lower Matanuska Valley; 3) there were readvances of the Matanuska Glacier >6 km from its current terminus to the vicinity of One Hundred Mile Lake (Williams and Ferrians, 1961; Fig. 2A) and of the Knik Glacier ~20 km back (Reger and Updike, 1983) to very nearly its previous

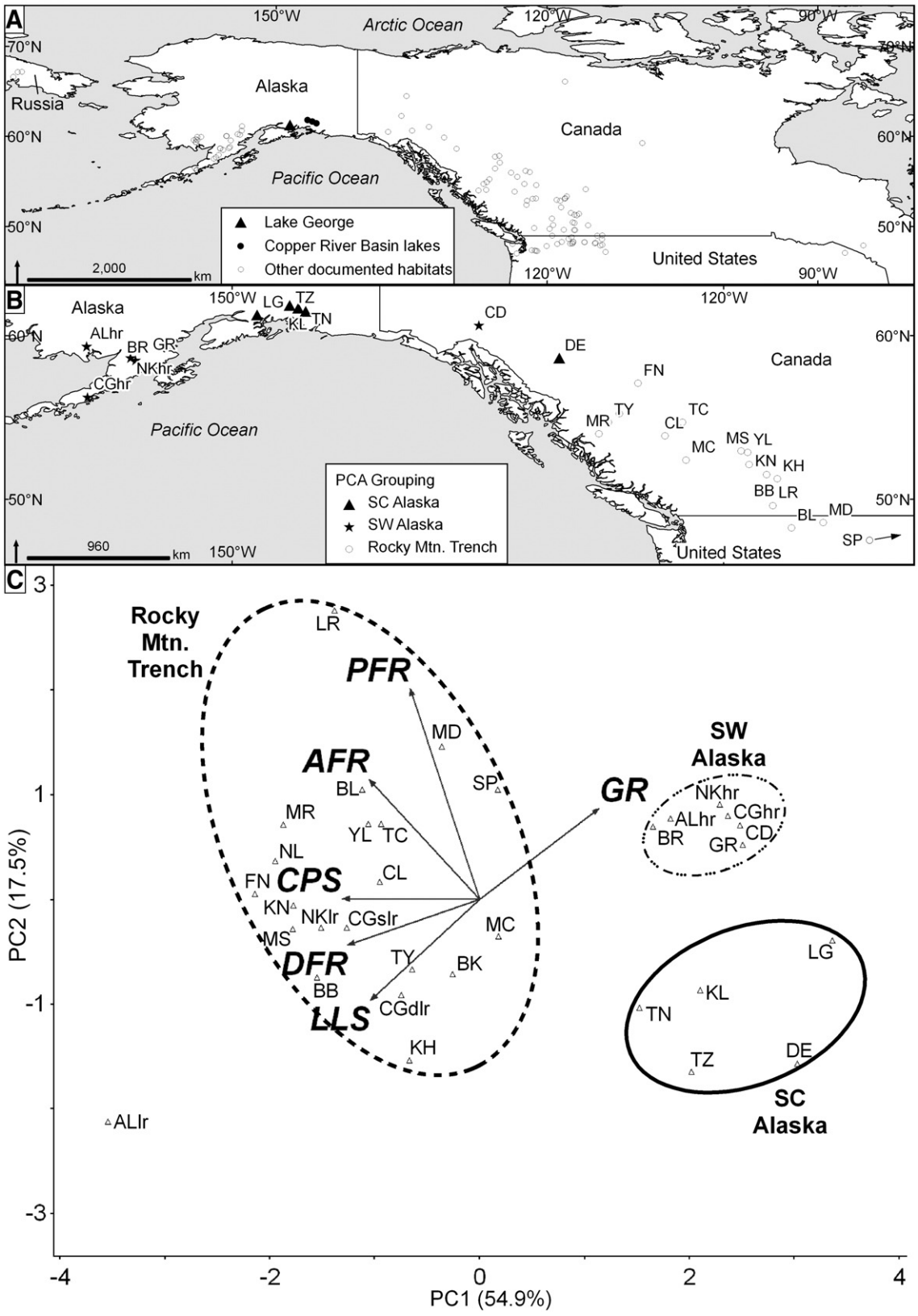

Figure 6. A: Pygmy whitefish *Prosopium coulterii* documented global distribution. B: Locations of North American pygmy whitefish collections for which meristic data is available (see Table 1 for details). Symbols represent three apparent groupings in multivariate space (Fig. 6C): solid triangles show Copper River Basin, Yukon/Mackenzie headwaters, and Lake George populations (south-central Alaska group); solid stars show south-west Alaska (presumptive ancestral populations only) and Yukon River populations (south-west Alaska group); open circles show British Columbia, Montana, and Lake Superior populations (Rocky Mountain Trench group). SU = Lake Superior population to east of map. C: First two principal components of a PCA (R Development Core Team, 2009) of six North American pygmy whitefish meristic characters (Table 1). The dashed line envelopes populations from the southeast extent of pygmy whitefish distribution, centered along the Rocky Mountain Trench; the dashed-dotted line envelopes populations from southwest Alaska and the Yukon River, and the solid line envelopes populations from Yukon/Mackenzie headwaters, Copper River Basin, and Lake George.

Table 1
North American pygmy whitefish meristic data. Records are for all locations with ≥4 observations of each of six meristic characters: $\overline{GR}$ = mean gillrakers, $\overline{LLS}$ = mean lateral line scales, $\overline{CPS}$ = mean caudal peduncle scales, $\overline{DFR}$ = mean dorsal fin rays, $\overline{AFR}$ = mean anal fin rays, $\overline{PFR}$ = pectoral fin rays. Abbreviation suffixes (slr = shallow water low-(gill) rakered, dlr = deep water low rakered, hr = high rakered, lr = low rakered) identify meristically, morphologically, and ecologically distinct sympatric forms in three southwestern Alaskan lakes described by McCart (1970).

Modern drainage	Locality	Abbreviation	Source	Latitude	Longitude	$\overline{GR}$	$\overline{LLS}$	$\overline{CPS}$	$\overline{DFR}$	$\overline{AFR}$	$\overline{PFR}$
Chignik	Black Lk.	BK	McCart (1970)	56.456	−158.991	14.06	61.54	17.54	11.25	11.81	15.19
Chignik	Chignik Lk.	CGslr	McCart (1970)	56.259	−158.824	14.16	63.95	18.02	11.36	12.44	15.40
Chignik	Chignik Lk.	CGdlr	McCart (1970)	56.259	−158.824	14.50	62.94	17.93	11.55	11.95	15.05
Chignik	Chignik Lk.	CGhr	McCart (1970)	56.259	−158.824	19.21	61.44	16.00	10.15	12.21	15.07
Columbia	Blaeberry R.	BB	McCart (1970)	51.519	−117.373	14.15	62.90	19.31	11.70	11.95	15.30
Columbia	Bull Lk.	BL	Eschmeyer and Bailey (1955)	48.251	−115.857	16.71	60.70	18.50	11.83	12.57	15.89
Columbia	Kicking Horse R.	KH	McCart (1970)	51.259	−116.723	14.66	61.75	18.75	11.58	12.00	14.33
Columbia	Kinbasket Lk.	KN	McCart (1970)	52.132	−118.436	13.60	60.15	18.07	12.05	12.65	15.40
Columbia	Laird Ck.	LR	McCart (1970)	49.621	−117.004	15.70	57.80	18.23	11.45	13.15	16.85
Columbia	Lake McDonald	MD	Eschmeyer and Bailey (1955)	48.583	−113.920	17.20	59.20	18.35	11.40	12.45	16.00
Copper River	Klutina Lk.	KL	Bird and Roberson (1979)	61.691	−145.966	17.50	55.50	16.00	11.40	11.90	13.90
Copper River	Tazlina Lk.	TZ	Bird and Roberson (1979)	61.858	−146.490	15.30	56.60	16.30	11.00	11.40	13.90
Copper River	Tonsina Lk.	TN	Bird and Roberson (1979)	61.500	−145.527	15.30	57.00	16.00	11.30	11.50	14.50
Fraser	Cluculz Lk.	CL	McCart (1970)	53.884	−123.585	13.70	58.59	18.88	11.15	12.55	15.26
Fraser	McLeese Lk.	MC	McCart (1970)	52.407	−122.296	15.80	54.95	18.63	11.75	11.90	14.70
Fraser	Moose Lk.	MS	McCart (1970)	52.962	−118.936	13.75	61.60	18.48	11.80	12.70	15.20
Fraser	Yellowhead Lk.	YL	McCart (1970)	52.867	−118.533	13.90	57.09	18.11	11.64	12.54	15.73
Knik	Lake George	LG	This study	61.280	−148.480	17.67	58.17	15.83	10.33	10.50	15.17
Mackenzie	Dease Lk.[1]	DE	McCart (1970)	58.633	−130.038	17.50	56.10	16.15	10.85	11.25	13.60
Mackenzie	Finlay R.	FN	McCart (1970)	56.879	−126.972	14.60	60.50	19.30	12.10	12.90	15.20
Mackenzie	Tacheeda Lk.	TC	McCart (1970)	54.719	−122.511	14.47	56.57	19.00	11.60	12.20	15.80
Naknek	Brooks Lk.	BR	McCart (1970)	58.513	−155.901	16.32	54.85	15.90	11.00	12.10	15.20
Naknek	Grosvenor Lk.	GR	McCart (1970)	58.684	−155.222	17.10	55.70	15.33	10.44	12.30	14.70
Naknek	Naknek Lk.	NKlr	McCart (1970)	58.649	−156.210	14.54	62.77	17.85	12.00	12.33	15.48
Naknek	Naknek Lk.	NKhr	McCart (1970)	58.649	−156.210	17.33	55.37	15.62	10.77	11.80	15.40
Nushagak	Lk. Aleknagik	ALlr	McCart (1970)	59.367	−158.893	13.46	71.57	19.91	12.11	12.80	14.51
Nushagak	Lk. Aleknagik	ALhr	McCart (1970)	59.367	−158.893	15.82	56.88	16.18	10.43	11.72	15.63
Saint Lawerence	Lake Superior	SP	Eschmeyer and Bailey (1955)	47.097	−87.007	18.28	57.14	19.46	10.90	13.20	14.62
Skeena	Morice Lk.	MR	McCart (1970)	54.005	−127.606	15.20	62.20	19.20	11.70	12.65	15.90
Skeena	Nilkitkwa Lk.	NL	McCart (1970)	55.241	−126.374	13.70	61.15	18.85	11.80	12.40	15.95
Skeena	Tyhee Lk.	TY	McCart (1970)	54.657	−126.925	14.30	61.90	19.20	11.10	11.70	15.25
Yukon	Chadburn Lk	CD	McCart (1970)	60.643	−134.947	19.00	54.29	17.00	11.00	11.43	15.14

Elmendorf Moraine position; 4) both glaciers retreated to their current positions.

Flood depth, velocity, discharge, and duration estimates

We estimated paleoflood parameters through the application of three approaches: 1) empirically derived dam-break and jökulhlaup discharge relationships with dam height and impounded lake volume, 2) Manning's equation to two bracketing flow depths, and 3) the Froude equation assuming critical flow and two bracketing flow depths. Baker et al. (1993) related peak discharge to the product of dam height and lake volume for both cataclysmic dam breaks [$Q_{cm} = 296(HV)^{0.51}$] and more gradual subglacial jökulhlaups [$Q_{jm} = 3.24(HV)^{0.62}$, where Q_{cm} and Q_{jm} = maximum cataclysmic and jökulhlaup discharges (10^6 m^3 s^{-1}), H = dam height (m), and V = decant volume (in units of 10^6 m^3)] (Table 4). Using these relationships, we estimated the peak discharge of the Matanuska Valley flood was 2.0–3.3 × 10^6 m^3 s^{-1} (dam break) or 1.5–2.7 × 10^5 m^3 s^{-1} (jökulhlaup). Similarly, we estimated the peak discharge for the Susitna River flood was 7.0–11.3 × 10^6 m^3 s^{-1} (dam break) or 0.7–1.2 × 10^6 m^3 s^{-1} (jökulhlaup). For reference, the largest recognized freshwater flood discharges are Missoula [≥17 × 10^6 m^3 s^{-1} (O'Connor and Baker, 1992)]; Kuray [10 × 10^6 m^3 s^{-1} (Herget, 2005)]; Lake Agassiz [2–7 × 10^6 m^3 s^{-1} (Smith, 2003)]; Tsangpo [5 × 10^6 m^3 s^{-1} (Montgomery et al., 2004)]; Yenisei [3.5 × 10^6 m^3 s^{-1} (Komatsu et al., 2009)]; Ulagan [1–2 × 10^6 m^3 s^{-1} (Rudoy, 2002)]; Aniakchak [1 × 10^6 m^3 s^{-1} (Waythomas et al., 1996)]; and Bonneville [1 × 10^6 m^3 s^{-1} (O'Connor, 1993)]. Only the largest estimated discharge from each locale is listed.

We estimated flow depths over the Wasilla-area VLD train using two approaches that constrain minimum and maximum values. Our minimum depth estimate of 34 m was constrained by the maximum height of the individual VLDs. We assumed the water surface slope for this modeled depth was the mean topographic slope (0.004). We also estimated the flow depths implied by the VLD train using Allen's (1968) relationship between dune height and flow depth, which predicts that flow depths declined from about 110 m at their upstream end to <45 m at their downstream end (Fig. 3). We take the value of 70 m at the midway point along the VLD train to be representative. We assumed the water surface slope for this modeled depth was that predicted by Allen's (1968) relationship (0.01, Fig. 3).

Table 2
Principal Component Analysis (PCA) pygmy whitefish meristic character eigenvectors.

Structure correlations (correlation coefficients cross-products matrix)						
	PC1	PC2	PC3	PC4	PC5	PC6
GR	0.769	−0.331	0.391	−0.218	0.255	−0.183
LLS	−0.705	0.367	−0.057	−0.591	−0.026	−0.122
CPS	−0.883	−0.002	0.172	0.000	0.354	0.254
DFR	−0.848	0.167	0.070	0.368	0.102	−0.319
AFR	−0.713	−0.435	0.456	−0.031	−0.303	0.031
PFR	−0.446	−0.768	−0.439	−0.091	0.070	−0.067

Table 3
Principal component eigenvalues and tests of significance.

Randomization test of eigenvalues (1000 randomizations):						
	PC1	PC2	PC3	PC4	PC5	PC6
Eigenvalue	3.296	1.052	0.592	0.542	0.299	0.220
Proportion of variance	0.549	0.175	0.099	0.090	0.050	0.037
Cumulative proportion	0.549	0.725	0.823	0.913	0.963	1.000
Broken-stick value	2.450	1.450	0.950	0.617	0.367	0.167
P-value	0.000	0.999	1.000	1.000	1.000	0.997

Even at this maximum flow depth, the decreasing calculated water surface elevation suggests flood flows spread laterally north into the Susitna Valley and south around the terminus of the Knik Glacier but did not overtop the central Elmendorf Moraine (Fig. 5).

Based on the constraining minimum and maximum flood depths of 34 and 70 m, we used the Manning and Froude equations to provide two independent estimates of the flood velocity (υ). Adopting the conventional wide-channel assumption that these flow depths approximate the hydraulic radius (R), together with an average slope (S) of 0.004 or 0.01, and an estimated roughness coefficient (n) of 0.04 ± 0.01 (Benito and O'Connor, 2003), the Manning equation [$\upsilon = R^{0.67} S^{0.5} / n$] yielded predicted flow velocities of 13 to 57 m/s. We also estimated the velocity of the flood by assuming that the flow was critical, and thus had a Froude number [$F_r = \upsilon / (gD)^{0.5}$] where g is gravitational acceleration and D is the flow depth] equal to 1. This resulted in estimated flow velocities of 18 to 26 m/s, a range within that predicted by the Manning equation. Baker et al. (1993) calculated that velocities for the catastrophic ice-dam-failure Kuray flood were up to 20 to 45 m/s. With our assumed 34-m depth and calculated velocity ranges, a 6.1-km-wide VLD train would have formed under discharges of 2.8×10^6 to $4.6 \times 10^6 m^3 s^{-1}$, which agrees well with

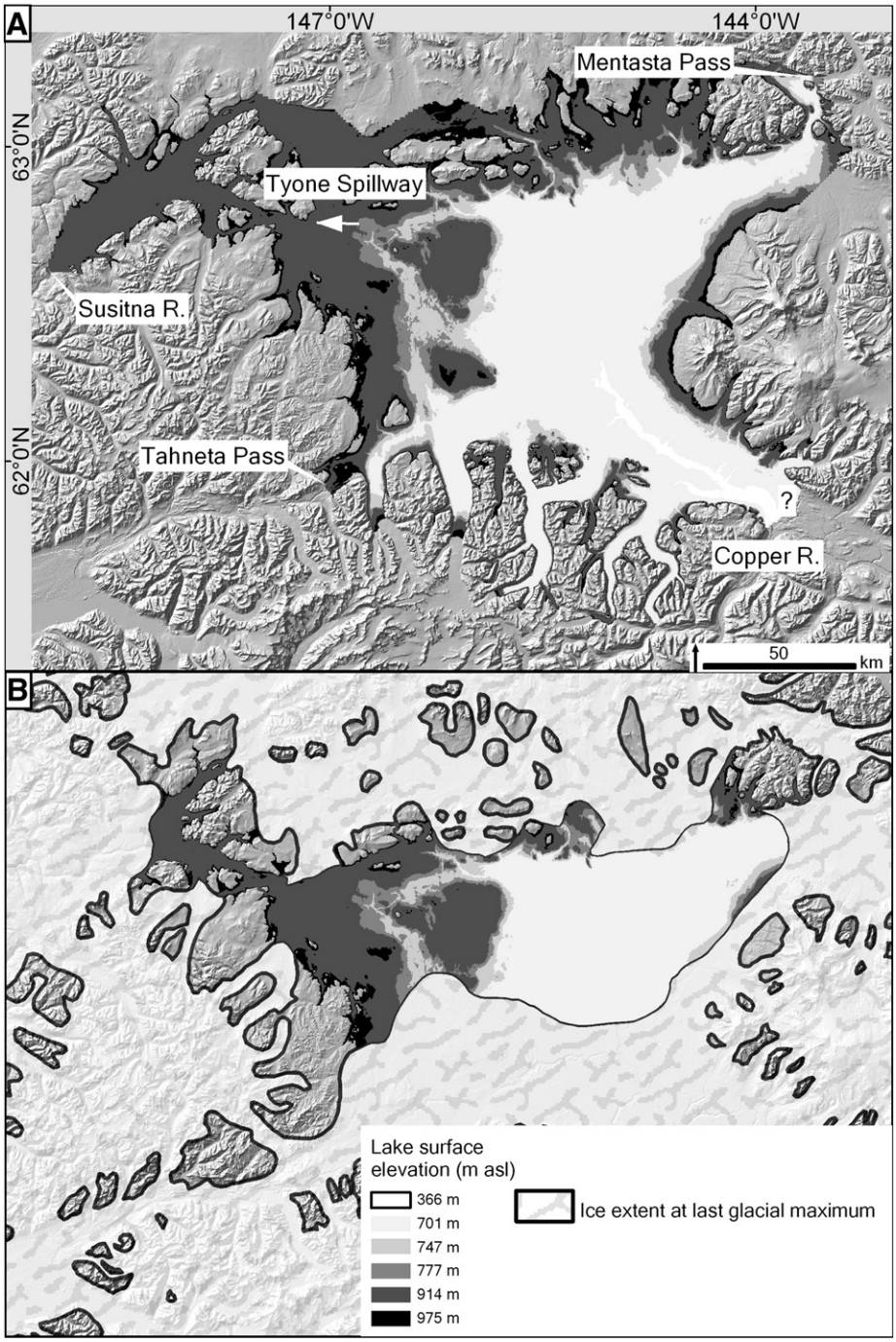

Figure 7. Lake Atna key surface-level reconstructions. Lake levels correspond to maximum recorded (975 m; Williams and Galloway, 1986), outlet-controlled (914, 777, 747, and 701 m amsl; Ferrians and Schmoll, 1957; Nichols and Yehle, 1969; Williams and Galloway, 1986), and lowest recorded (366 m amsl; Nichols and Yehle, 1969) surface elevations. A: Maximum possible lake extent for each shoreline elevation based on ice-free topography and inferred ice dams. B: Minimum lake extent based on location of CRB ice front at the LGM (Manley et al., 2002); the 366-m amsl lake surface is not displayed as it would have been entirely subglacial.

Table 4
Lake Atna characteristics for different paleolake levels, keyed to spillway elevations, and estimated volumes, discharges, and durations for catastrophic outbursts and jökulhlaups. Pre- and post-decant lake surface elevations based on previous work; minimum and maximum lake extent parameters based on DEM analyses. Only the presumptive last drainage from lowest mapped shoreline (Nichols and Yehle, 1969) down the Copper River is estimated; earlier, perhaps much larger, Copper River discharges may have occurred. Uncertainty of the Chitina Valley glacier terminus location (query in Fig. 7A) has greatest influence on our estimates of the last flood down the Copper River.

Outlet	Lake surface elevation (m amsl)		Initial area (10^3 km^2)	Initial volume (10^3 km^3)	Dam height (m)	Decant volume (10^3 km^3)	Maximum discharge (10^6 m^3 s^{-1})		Duration (Days)	
	Pre-flood	Post-flood					Jökulhlaup	Catastrophic failure	Jökulhlaup	Catastrophic failure
Tahneta Pass	975	914	8.9–24.0	2.3–6.0	61	0.5–1.4	0.1–0.3	2.0–3.3	83–121	6–10
Susitna River	914	777	8.3–21.6	1.7–4.6	346	1.0–2.6	0.7–1.2	7.0–11.3	36–51	3–5
Mentasta Pass	747	701	4.6–11.5	0.5–1.6	46	0.2–0.5	0.07–0.1	1.0–1.6	68–96	4–7
Copper River	366	160	0.4	0.03	206	0.03	0.05	0.8	13	1

the dam-break-model result. With our assumed 70-m depth and calculated velocities, a 9-km-wide channel would have conveyed discharges of 16.5×10^6 to 36.2×10^6 m^3 s^{-1}, which far exceed the dam-break model result. Although the close agreement between the Manning and Froude equation results and the cataclysmic dam-break model estimate suggests that the lower water depth should be preferable, the potential for a flood release from Lake Atna to incorporate elements of the Matanuska Glacier downstream from the Tahneta Pass dam allows the possibility that the flood discharge grew as it progressed down-valley before shaping the VLD train.

O'Connor et al. (2002) approximated flood duration by $t = V\times 0.5Q_m^{-1}$, where t = time, V = volume, and Q_m = peak discharge. From this, we estimated, based on the cataclysmic dam-break and jökulhlaup models of Baker et al. (1993), the duration of the Matanuska Valley flood would have been 6–10 days for a dam break or 80–120 days for a jökulhlaup. We estimated that the duration for the Susitna River flood would have been 6–9 days for a dam break or 65–90 days for a jökulhlaup.

Summary and conclusions

Multiple lines of evidence support a ~15.5–26 ka megaflood from glacial Lake Atna down the Matanuska Valley to Upper Cook Inlet. First, reported Lake Atna levels reached ~60 m above the pass between the CRB and the Matanuska River. Maximum elevations of the broad flow path (~975 m amsl) and incised channel banks (~914 m amsl) through Tahneta Pass match Lake Atna's maximum reported and highest prolonged surface elevations. Second, the lack of expected till and the presence of fluvially streamlined islands in the middle Matanuska Valley suggest large scouring flows. Third, ~25 prominent flow-transverse very large dunes, with 0.9-km chord lengths, heights to 34 m, built of steeply dipping foresets, and with superposed smaller dunes, indicate flood flows ≤110 m deep in the lower Matanuska Valley. Fourth, thick marine/estuarine deposits opposite the flood path mouth include a thin clay and silt stratum with open-flocculated "card-house" microfabric with interstitial freshwater, the failure of which led to lethal 1964 Alaskan earthquake

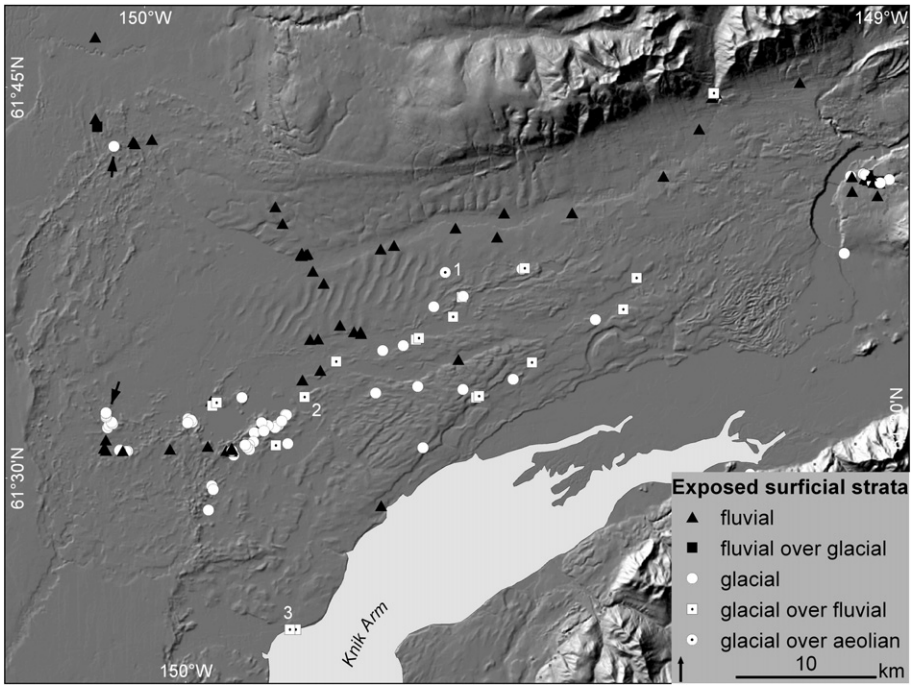

Figure 8. Lower Matanuska Valley surficial substrates (excluding Holocene deposits) [data from Reger et al. (1996) and this study]. Surficial glacial deposits mark the location of the Knik Glacier during the flood and its post-flood resurgence. Glacial deposits (black arrows) on the northwest terminal Elmendorf Moraine and southwest recessional moraine represent sites apparently not overtopped by the flood. We interpret the glacial over aeolian and fluvial over aeolian (symbol concealed) deposits at Site 1 as Knik Glacier readvance and outwash over aeolian deposits in the Matanuska flood path, indicating subaerial conditions after the flood and before the Knik Glacier readvance. We interpret the glacial drift containing clasts, apparently from the Knik Valley (C. Hults, USGS, Anchorage, personal communication, 2009), over fluvial deposits dominated by clasts from the Matanuska Valley at sites (e.g., Site 2) in and adjacent to the paleochannel as evidence of post-flood resurgence of Knik Glacier west and southwest (e.g., Site 3) to the southern lobe of the Elmendorf Moraine.

landslides. Fifth, modern Lake George, adjacent to the Matanuska Valley, provides the only known Cook Inlet basin habitat for the nonanadromous pygmy whitefish. Meristic characters suggest that pygmy whitefish of Lake George and three Lake Atna relict lakes are more closely related to each other than they are to other extant populations, indicating ancestral Lake George and Lake Atna shared a freshwater connection. Lake Atna's size, ~50 ka duration, and sequential connection to four major drainages likely made it an important late Pleistocene freshwater refugium.

We conclude that $\leq 1400\,km^3$ of Lake Atna decanted through Tahneta Pass, at a rate of $\geq 3\times10^6\,m^3\,s^{-1}$. If the Matanuska megaflood was initiated by catastrophic ice dam failure, as indicated by the scale of the VLDs near Wasilla, then it appears to have been among the largest freshwater peak discharges known. A later discharge down the Susitna River may have been 3–4 times greater, making glacial Lake Atna a serial generator of some of Earth's largest freshwater floods.

Acknowledgments

Field work in 2008 was supported by the University of Washington's Quaternary Research Center and aided by G. Wiedmer; 2009 analysis was supported by the University of Washington's College of Forest Resources and a Reed Fellowship to MW. Lake George fish assemblage sampling and analysis was inspired by S. Hayes, assisted by J. Buckwalter, T. Pietsch, and K. Pearson Maslenikov, and supported by U.S. Fish and Wildlife Service State Wildlife Grant T-1-14 (P-10) to MW while at the Alaska Department of Fish and Game. We thank T. Cox, Natural Resources Conservation Service, for QuickBird imagery, M. Logsdon and J. Olden for technical approaches, and J. Gale, L. Holmes, and the residents of the Matanuska-Susitna Borough for their help and understanding. S. Kopczynski shared generously her experience and unpublished Matanuska-Knik area data. We thank R. Reger, J. Curran, M. Gracz, R. Waitt, T. Hamilton, F. Wilson, C. Hults, C. Torgersen, and B. Sheets for their help strengthening early drafts. We thank V. Baker, R. Brown, and G. Komatsu for insightful recommendations that greatly improved the manuscript.

References

(ADF&G) Alaska Department of Fish and Game. 2009a. Alaska Freshwater Fish Inventory, http://www.sf.adfg.state.ak.us/SARR/Surveys/index.cfm. Alaska Department of Fish and Game, Division of Sport Fish.

(ADF&G) Alaska Department of Fish and Game. 2009b. Lake Maps Series, http://www.sf.adfg.state.ak.us/statewide/lakedata/. Alaska Department of Fish and Game, Division of Sport Fish.

AFS (Alaska Fire Service), 1999. Historical fire perimeters. Bureau of Land Management, Alaska Fire Service.

Ager, T.A., Brubaker, L., 1985. Quaternary palynology and vegetational history of Alaska. In: Bryant, V.M., Holloway, R.G. (Eds.), Pollen Records of late-Quaternary North American Sediments: American Association of Stratigraphic Palynologists Foundation, pp. 353–384.

Allen, J.R.L., 1963. Asymmetrical ripple marks and the origin of water-laid cosets of cross-strata. Liverp. Manch. Geol. J. 3 (Part 2), 187–236.

Allen, J.R.L., 1968. Current Ripples; Their Relation to Patterns of Water and Sediment Motion. North-Holland Pub. Co.

Allen, J.R.L., Collinson, J.D., 1974. The superimposition and classification of dunes formed by unidirectional aqueous flows. Sed. Geol. 12, 169–178.

Ashley, G.M., 1990. Classification of large-scale subaqueous bedforms; a new look at an old problem. J. Sed. Res. 60 (1), 161–172.

Baker, V.R., 1978. Large-scale erosional and depositional features of the Channeled Scabland. In: Baker, V.R., Nummedal, D. (Eds.), The Channeled Scabland: A Guide to the Geomorphology of the Columbia Basin, Washington. Prepared for the Comparative Planetary Geology Field Conference held in the Columbia Basin, June 5–8, 1978. : Planetary Geology Program, Office of Space Science. NASA, pp. 81–115.

Baker, V.R., Benito, G., Rudoy, A.N., 1993. Paleohydrology of Late Pleistocene superflooding, Altay Mountains, Siberia. Science 259 (5093), 348–350.

Barton, L.H., Barrett, B.M., 1973. Cook Inlet inventory report, 1973; Cook Inlet data report no. 73-6. Alaska Department of Fish and Game, Division of Commercial Fisheries.

Benito, G., O'Connor, J.E., 2003. Number and size of last-glacial Missoula floods in the Columbia River valley between the Pasco Basin, Washington, and Portland, Oregon. Geol. Soc. Am. Bull. 115 (5), 624–638.

Bill, D.L., Namtvedt, T.B., Davis, A.S., 1972. Cook Inlet lake and stream inventory, 1972. Progress report. Alaska Department of Fish and Game, Division of Commercial Fisheries.

Bird, F.H., Roberson, K., 1979. Pygmy whitefish, *Prosopium coulteri*, in three lakes of the Copper River System in Alaska. J. Fish. Res. Board Can. 36, 468–470.

Bjerrum, L., 1954. Geotechnical properties of Norwegian marine clays. Geotechnique 4, 49–69.

Bretz, J.H., 1923. The channeled scablands of the Columbia Plateau. J. Geol. 31 (8), 617–649.

Bretz, J.H., Smith, H.T.U., Neff, G.E., 1956. Channeled scabland of Washington; new data and interpretations. Geol. Soc. Am. Bull. 67, 957–1049.

Briner, J.P., 2005. Do long subglacial bedforms indicate fast ice flow? A case study from New York. Abstr. Programs, Geol. Soc. Am. 37, 22.

Buell, J. 1991. Alaska Freshwater Fish Inventory report: Retrieved 08/13/2009 from http://gis.sf.adfg.state.ak.us/fishsurv_IMS/Reports/rptStation.cfm?sid=-PEB91CH007. Alaska Department of Fish and Game, Division of Sport Fish.

Carling, P.A., 1989. Hydrodynamic models of boulder berm deposition. Geomorphology 2, 319–340.

Carson, M.A., 1981. Influence of porefluid salinity on instability of sensitive marine clays; a new approach to an old problem. Earth Surf. Process. Land. 6, 499–515.

Chereshnev, I.A., Skopets, M.B., 1992. A new record of the pygmy whitefish, *Prosopium coulteri*, from the Amguem River Basin, (Chukotski Peninsula). J. Ichthyol. 32 (4), 46–55.

Danzeglocke, U., Jöris, O., Weninger, B. 2010. CalPal-2007online. http://www.calpal-online.de/, accessed 2010-03-09.

Eigenmann, C.H., Eigenmann, R.S., 1892. New fishes from western Canada. Am. Nat. 26 (311), 961–964.

Eschmeyer, P.H., Bailey, R.M., 1955. The pygmy whitefish, *Coregonus coulteri*, in Lake Superior. Trans. Am. Fish. Soc. 84, 161–199.

Ferrians, O.J., 1984. Pleistocene glacial history of the northeastern Copper River Basin, Alaska. Geol. Soc. Am. Abstr. Programs 16, 282.

Ferrians Jr., O.J., Schmoll, H.R., 1957. Extensive proglacial lake of Wisconsin age in the Copper River Basin, Alaska. Geol. Soc. Am. Bull. 68 (12, Part 2), 1726.

Fisher, T.G., Shaw, J., 1992. A depositional model for Rogen moraine, with examples from the Avalon Peninsula, Newfoundland. Can. J. Earth Sci. 29 (4), 669–686.

Froese, R., Pauly, D., 2009. FishBase, World Wide Web electronic publication www.fishbase.org (accessed 04/2009).

Gupta, S., Collier, J.S., Palmer-Felgate, A., Potter, G., 2007. Catastrophic flooding origin of shelf valley systems in the English Channel. Nature 448 (7151), 342–345.

Hallock, M., Mongillo, P.E., 1998. Washington State Status Report for the Pygmy Whitefish. Washington Department of Fish and Wildlife.

Heard, W.R., Hartman, W.L., 1966. Pygmy whitefish *Prosopium coulteri* in the Naknek River system of southwest Alaska. Fish. Bull. Fish Wildl. Serv. 65, 555–579.

Herget, J., 2005. Reconstruction of Pleistocene ice-dammed lake outburst floods in the Altai Mountains, Siberia. Spec. Pap. Geol. Soc. Am. 386.

Kerr, M., Eyles, N., 2007. Origin of drumlins on the floor of Lake Ontario and in upper New York State. Sed. Geol. 193, 7–20.

Komar, P.D., 1983. Shapes of streamlined islands on Earth and Mars: experiments and analyses of the minimum-drag form. Geology 11, 651–654.

Komatsu, G., Arzhannikov, S.G., Gillespie, A.R., Burke, R.M., Miyamoto, H., Baker, V.R., 2009. Quaternary paleolake formation and cataclysmic flooding along the upper Yenisei River. Geomorphology 104, 143–164.

Kopczynski, S.E., 2008. Satellite predictions of subglacial hydrology and final collapse of twinned terrestrial·tidewater glaciers, Anchorage lowland, Alaska. Unpublished Ph.D. thesis, Lehigh University.

Kostaschuk, R., Villard, P., 1996. Flow and sediment transport over large subaqueous dunes: Fraser River, Canada. Sedimentology 43 (5), 849–863.

Lambe, T.W., 1958. The structure of compacted clay. Proc. Am. Soc. Civil Eng. 84 (SM2), 1–34.

Lindsey, C.C., Franzin, W.G., 1972. New complexities in zoogeography and taxonomy of pygmy whitefish (*Prosopium coulteri*). J. Fish. Res. Board Can. 29 (12), 1772–1775.

Lonzarich, D., 1992. The University of Washington Burke Museum Fish Collection online search engine at: http://biology.burke.washington.edu/ichthyology/database/search.php.

Lundqvist, J., 1989. Rogen (ribbed) moraine—identification and possible origin. Sed. Geol. 62 (2–4), 281–292.

Mackay, W.C., 2000. Status of the pygmy whitefish (*Prosopium coulteri*) in Alberta, Alberta Environment, Fisheries and Wildlife Management Division, and Alberta Conservation Association, Wildlife Status Report No. 27.

Manley, W.F., et al., 2002. Alaska paleoglacier atlas. Geol. Soc. Am. Abstr. Programs 34 (6), 548.

Mathisen, O.A., Sands, N.J., 1999. Ecosystem modeling of Becherof Lake, a sockeye salmon nursery lake in Southwestern Alaska. Ecosystem Approaches for Fisheries Management: Proceedings of the Symposium on Ecosystem Considerations in Fisheries Management, September 30–October 3, 1998, Anchorage, Alaska. University of Alaska Sea Grant Program, pp. 685–703.

Mayhood, D.W., 1992. A preliminary assessment of the native fish stocks of Jasper National Park; Part 3 of a Fish Management Plan for Jasper National Park. Canadian Parks Service, Jasper National Park.

McCart, P., 1970. Evidence for the existence of sibling species of pygmy whitefish (*Prosopium coulteri*) in three Alaskan lakes. In: Lindsey, C.C., Woods, C.S. (Eds.), Biology of Coregonid Fishes. University of Manitoba Press, pp. 81–98.

Montgomery, D.R., Hallet, B., Yuping, L., Finnegan, N., Anders, A., Gillespie, A., Greenberg, H.M., 2004. Evidence for Holocene megafloods down the Tsangpo River gorge, southeastern Tibet. Quatern. Res. 62, 201–207.

Myers, G.S., 1932. A New Whitefish, Prosopium snyderi, from Crescent Lake, Washington. Copeia 1932 (2), 62–64.

Nelson, J.S., Shelast, B., 1998. Pygmy whitefish in the Athabasca River near Whitecourt, Alberta. Ab Nat. 28 (3), 59–60.

Nichols, D.R., 1965. Glacial history of the Copper River Basin. In: Péwé, T.L. (Ed.), International Association for Quaternary Research, VIIth Congress. Nebraska Academy of Sciences, p. 360.

Nichols, D.R., Yehle, L.A., 1969. Engineering geologic map of the southeastern Copper River Basin, Alaska: U.S. Geological Survey Miscellaneous Investigations 524, 1 sheet, scale 1:125,000. USGS.

O'Connor, J.E., 1993. Hydrology, hydraulics, and geomorphology of the Bonneville flood. Geol. Soc. Am. Spec. Pap. 274, 1–83.
O'Connor, J.E., Baker, V.R., 1992. Magnitudes and implications of peak discharges from glacial Lake Missoula. Geol. Soc. Am. Bull. 104 (3), 267–279.
O'Connor, J.E., Grant, G.E., Costa, J.E., 2002. The geology and geography of floods. In: House, P.K., Webb, R.H., Baker, V.R., Levish, D.R. (Eds.), Ancient Floods, Modern Hazards: Principals and Application of Paleoflood Hydrology: American Geophysical Union Water Science and Application Series no. 5. , pp. 359–385.
Plumb, M.P., 2006. Ecological factors influencing fish distribution in a large subarctic lake system. M.S. thesis, University of Alaska.
Poe, P.H., Cortner, G.D., Mathisen, O.A., 1976. Monitoring of the Kvichak spawning and nursery areas in 1975; Final Report, Contract No. 2131, Fisheries Research Institute, College of Fisheries, University of Washington.
R Development Core Team, 2009. R: A Language and Environment for Statistical Computing. R Foundation for Statistical Computing http://www.R-project.org.
R & M Consultants, Inc., 1981. Terrain unit maps, photointerpretation, subtask 5.02. Report on Susitna Hydroelectric Project, Alaska Power Authority 1980–81, Geotechnical Report v. 2, Appendix J, Final Draft. Acres Inc.
Rankin, L., 2004. Phylogenetic and ecological relationship between giant pygmy whitefish (*Prosopium spp.*) and pygmy whitefish (*Prosopium coulteri*) in north-central British Columbia. M.S. thesis, The University of Northern British Columbia.
Reger, R.D., Hubbard, T.D., 2009. Evidence for Late Wisconsinan outburst floods in the Tok-Tanacross Basin, Upper Tanana River valley, east-central Alaska. Geol. Soc. Am. Abstr. Programs 41 (7), 637.
Reger, R.D., Updike, R.G., 1983. Physiographic map and field-trip localities of the Upper Cook Inlet area, Alaska. In: Péwé, T.L., Reger, R.D. (Eds.), Guidebook to Permafrost and Quaternary Geology along the Richardson and Glenn Highways Between Fairbanks and Anchorage, Alaska. : Fourth International Conference on Permafrost. American Geophysical Union.
Reger, R.D., Combellick, R.A., Brigham-Grette, J., 1995. Late-Wisconsin events in the Upper Cook Inlet region, Southcentral Alaska. In: Combellick, R.A., Tannian, F. (Eds.), Short Notes on Alaska Geology 1995: Professional Report 117. Alaska Division of Geological & Geophysical Surveys, pp. 33–45.
Reger, R.D., Pinney, D.S., Burke, R.M., Wiltse, M.A., 1996. Catalog and initial analyses of geologic data related to Middle to Late Quaternary deposits, Cook Inlet region, Alaska: Alaska Division of Geological & Geophysical Surveys Report of Investigation 95-6, Fairbanks, AK.
Reger, R.D., Sturmann, A.G., Berg, E.E., Burns, P.A.C., 2008. A guide to the late Quaternary history of northern and western Kenai Peninsula, Alaska; Guidebook 8. Alaska Division of Geological & Geophysical Surveys.
Reimer, P.J., et al., 2004. IntCal04 terrestrial radiocarbon age calibration, 0–26 cal kyr BP. Radiocarbon 46 (3), 1029–1058.
Roberson, K., Bird, F.H., Fridgen, P.J., Zorich, R.G., 1978. Copper River-Prince William Sound sockeye salmon catalog and inventory. Annual Completion Report AFC-52-3. Alaska Department of Fish and Game.
Rubin, M., Alexander, C., 1960. U.S. Geological Survey radiocarbon dates V. Radiocarbon 2, 129–185.
Rudoy, A.N., 2002. Glacier-dammed lakes and geological work of glacial superfloods in the Late Pleistocene, Southern Siberia, Altai Mountains. Quatern. Int. 87, 119–140.
Rudoy, A.N., Baker, V.R., 1993. Sedimentary effects of cataclysmic Late Pleistocene glacial outburst flooding, Altay Mountains, Siberia. Sed. Geol. 85, 53–62.
Russell, R., 1980. A fisheries inventory of waters in the Lake Clark National Monument Area. Alaska Department of Fish and Game, Division of Sport Fish, King Salmon, AK.
Schmoll, H.R., 1984. Late Pleistocene morainal and glaciolacustrine geology in the Upper Copper River-Mentasta Pass area, Alaska. Geol. Soc. Am. Abstr. Programs 16 (5), 332.
Schmoll, H.R., Yehle, L.A., Updike, R.G., 1999. Summary of Quaternary geology of the Municipality of Anchorage, Alaska. Quatern. Int. 60 (1), 3–36.
Schrader, F.C., 1900. A reconnaissance of a part of Prince William Sound and the Copper River district, Alaska, In: U. S. Geological Survey 20th Annual Report, 1898–99, Pt. VII-Exploration in Alaska in 1898. Department of the Interior, U. S. Geological Survey, Government Printing Office, 341–423.
Smith, D., 2003. Late Pleistocene glacial Lakes McConnell and Mackenzie and the northwest outlet flood from glacial Lake Agassiz; their paleo environments in northeast Alberta and the Northwest Territories. Reservoir 30, 14.
Teller, J.T., Leverington, D.W., Mann, J.D., 2002. Freshwater outbursts to the oceans from glacial Lake Agassiz and their role in climate change during the last deglaciation. Quatern. Sci. Rev. 21 (8–9), 879–887.
Thorson, R.M., 1989. Late Quaternary paleofloods along the Porcupine River, Alaska: implications for regional correlation. In: Carter, L.D., Hamilton, T.D., Galloway, J.P. (Eds.), Late Cenozoic history of the Interior Basins of Alaska and the Yukon: U. S. Geological Survey Circular 1026. U. S. Government Printing Office, pp. 51–54.
Thorson, R.M., Dixon, E.J., Smith, G.S., Batten, A.R., 1981. Interstadial proboscidean from south-central Alaska: implications for biogeography, geology, and archeology. Quatern. Res. 16 (3), 404–417.
Torrance, J.K., 1979. Post-depositional changes in the pore-water chemistry of the sensitive marine clays of the Ottawa area, eastern Canada. Eng. Geol. 14, 135–147.
Trainer, F.W., 1953. Preliminary Report on the Geology and Ground-Water Resources of the Matanuska Valley Agricultural Area. U.S. Geological Survey Circular, Alaska, p. 268. 1 sheet.
Updike, R.G., Carpenter, B.A., 1986. Engineering Geology of the Government Hill Area, Anchorage. Bulletin, Alaska, p. 1588. USGS.
Updike, R.G., Ulery, C.A., 1986. Engineering-geologic map of southwest Anchorage, Alaska: Alaska Division of Geological & Geophysical Surveys Professional Report 89, 1 sheet, scale 1:15, 840.
Updike, R.G., Olsen, H.W., Schmoll, H.R., Kharaka, Y.K., Stokoe II, K.H., 1988. Geologic and geotechnical conditions adjacent to the Turnagain Heights Landslide, Anchorage. Bulletin, Alaska, p. 1817. USGS.
Waitt, R.B., Denlinger, R.P., O'Connor, J.E., 2009. Many monstrous Missoula floods down Channeled Scabland and Columbia Valley. Geol. Soc. Am. Field Guide 15, 775–844.
Walker, K.N., Yu, Z., Evenson, E.B., 2005. Abrupt change in atmospheric circulation in the early Holocene inferred from a calcite oxygen-isotope record from a marl lake in south-central Alaska. Geol. Soc. Am. Abstr. Programs 37 (1), 24.
Waythomas, C.F., Walder, J.S., McGimsey, R.G., Neal, C.A., 1996. A catastrophic flood caused by drainage of a caldera lake at Aniakchak Volcano, Alaska, and implications for volcanic hazards assessment. Geol. Soc. Am. Bull. 108 (7), 861–871.
Weisel, G.F., Hanzel, D.A., Newell, R.L., 1973. Pygmy whitefish, *Prosopium coulteri*, in western Montana. Fish. Bull. 71 (2), 587–596.
Williams, J.R., 1986. New radiocarbon dates from the Matanuska Glacier bog section. In: Bartsch-Winkler, S.B., Reed, K.M. (Eds.), Geologic Studies in Alaska by the U. S. Geological Survey During 1985. : Circular, vol. 978. USGS, pp. 85–88.
Williams, J.R., 1989. A working glacial chronology for the western Copper River Basin, Alaska. In: Carter, L.D., Hamilton, T.D., Galloway, J.P. (Eds.), Late Cenozoic History of the Interior Basins of Alaska and the Yukon. : Circular, vol. 1026. USGS, pp. 81–85.
Williams, J.R., Ferrians Jr., O.J., 1961. Late Wisconsin and recent history of the Matanuska Glacier, Alaska. Arctic 14 (2), 82–90.
Williams, J.R., Galloway, J.P., 1986. Map of western Copper River Basin, Alaska, showing lake sediments and shorelines, glacial moraines, and location of stratigraphic sections and radiocarbon-dated samples. Open-File Report 86-390, 30 p., 1 sheet, scale 1:250,000. USGS.
Winkler, G.R., 1992. Geologic map and summary geochronology of the Anchorage 1° x 3° quadrangle, southern Alaska: Miscellaneous Investigations Series Map I-2283, 1 sheet, scale 1:250,000. USGS.
Woodley, M.A., 1996. An investigation of pore water in Champlain Sea deposits at Mer Bleue, Ottawa, Canada. M.S. thesis, Carleton University.
Wynne-Edwards, V.C., 1947. The Yukon Territory. Bull. Fish. Res. Board Can. 72, 6–20.
Zemlak, R.J., McPhail, J.D., 2006. The biology of pygmy whitefish, *Prosopium coulterii*, in a closed sub-boreal lake: spatial distribution and diel movements. Environ. Biol. Fish. 76 (2–4), 317–327.